Electronic Supplementary Material (ESI) for Physical Chemistry Chemical Physics.
This journal is © the Owner Societies 2024

Supporting Information

Improved Structure Stability and Performance of $LiFeSO_4F$ Cathode Material for Lithium–Ion Batteries by Magnesium Substitution

Zhendong Guo[ab], Tieyang Wang[a], Mingchen Ni[b], Fenhong Song[a], Jing Fan[a], Xiaorui Dong[b*], Dashuai Wang[c*]

a. College of Energy and Power Engineering, Northeast Electric Power University, Jilin 132012, PR China
b. College of Science, Northeast Electric Power University, Jilin 132012, PR China
c. Institute of Zhejiang University-Quzhou, Quzhou 324000, PR China

***Corresponding authors: xiaoruidong@yeah.net (X.R. Dong)**
dswang@zju.edu.cn (D.S. Wang)

Experimental

1 Preparation of $LiFeSO_4F$ and Mg-substituted $LiFeSO_4F$ composites

Tavorite $LiFeSO_4F$ was prepared by a tetraethylene glycol (TEG) assisted solvothermal method. For the first step, $FeSO_4.H_2O$ was prepared by heating $FeSO_4.7H_2O$ at 100 °C for 3 h in an Ar/H_2 (93:7) atmosphere. The $FeSO_4.H_2O$ precursor was mixed with stoichiometric LiF and then ball-milled for 24 h in acetone. Mg-substituted $LiFeSO_4F$ was prepared by using stoichiometric amounts of a mixed-metal sulfate monohydrate precursor $(Fe_{1-x}Mg_x)SO_4•H_2O$ as precursor. The mixture was transferred into a 43 mL Teflon-lined steel autoclave along with 30 mL of TEG. The autoclave was kept at 260 °C for 60 h to allow the solvothermal reaction. After it was cooled to room temperature naturally, the resulting white−gray powders were washed with acetone several times and then dried in vacuum-oven at 60 °C. The $LiFeSO_4F$ and Mg-substituted $LiFeSO_4F$ samples with different substituted amount were labeled as LFS and LMFS-2 and LMFS-4, respectively.

2 Materials Characterizations

The crystal structures of the materials were studied by X-ray diffraction (XRD) on a Bruker AXS D8 diffractometer with Cu Kα radiation. The morphologies of the materials were observed by scanning electron microscope (SEM, JSM-6700F) amd transmission electron microscope (TEM, FEI Tecnai G2), respectively. X-ray photoelectron spectroscopy (XPS) was performed on an ESCALAB spectrometer using Mg−Kα light source. The AC impedance spectroscopy was performed on a Solartron 1260 impedance analyzer. Mössbauer spectroscopy was collected in the

transmission mode using a 57Co/Pd γ-ray source. Velocity calibration was performed with the data of α-Fe at room temperature. The element dissolution test the samples were also measured on an Agilent 725 radially-viewed ICP-OES instrument

3 Calculations

First-principles calculations were performed in the framework of density functional theory (DFT), as implemented in the Vienna ab initio simulation package (VASP). [1] The exchange correlation energy was described by the generalized gradient approximation (GGA) in the scheme proposed by Perdew-Burke-Ernzerhof (PBE). [2] The projector augmented wave (PAW) [3] potential was used with a planewave cutoff energy of 450 eV, and a 2 × 2 × 3 grid was used for the integration over the Brillouin zone, which was enough for convergence of energy. Considering the strong correlation in iron and magnesium elements, electronic structure calculations were performed by using a GGA plus Hubbard U (GGA+U) method, [4] where U=4.0 eV was used for the calculations. The spin-polarized method was considered in the calculations. The Bond Valence (BV) Model[5] [6] was used to analyze the Li ion diffusion pathways, and the climbing-image nudged elastic band (CI-NEB) method[7] was used to analyze the Li ion diffusion energy barriers in the structure. The geometry optimizations were performed by using the conjugated gradient method, and the convergence threshold was set as 1×10^{-5} eV/atom in energy and 0.01 eV/Å in force.

4 Electrochemical measurements

Electrochemical experiments were conducted on CR2032 coin cells using metallic lithium as the anode. The cathode slurry was composed of 70 wt.% active

material, 20 wt.% active carbon and 10 wt.% polyvinylidenefluoride binder which was pasted on an Al current collector. The anode and cathode were separated by a Celgard 2400 membrane. A 1 mol L^{-1} lithium hexafluorophosphate ($LiPF_6$) solution dissolving in ethylene carbonate (EC) and diethyl carbonate (DEC) (EC : DEC = 1: 1) was used as the electrolyte. Galvanostatic charge-discharge was performed on a LAND-2010 automatic battery tester in the voltage window of 2.5-4.5 V. Cyclic voltammetry (CV) and electrochemical impedance spectroscopy (EIS) were performed on a Bio-Logic VSP multichannel potentiostatic-galvanostatic system. The CV curves were collected using a voltage scan rate of 0.1- mV s^{-1}. The impedance data were recorded by applying an ac voltage of 5 mV in the frequency range from 1 MHz to 1 mHz.

Reference

1. G. Kresse and J. Furthmüller, *Phys. Rev. B*, 1996, **54**, 11169-11186.
2. J. P. Perdew, K. Burke and M. Ernzerhof, *Physical Review Letters*, 1996, **77**, 3865-3868.
3. P. E. Blöchl, *Phys. Rev. B*, 1994, **50**, 17953-17979.
4. A. I. Liechtenstein, V. I. Anisimov and J. Zaanen, *Phys. Rev. B*, 1995, **52**, R5467-R5470.
5. I. D. Brown, *Chem. Rev.*, 2009, **109**, 6858-6919.
6. J. Gao, G. Chu, M. He, S. Zhang, R. Xiao, H. Li and L. Chen, *Science China Physics, Mechanics & Astronomy*, 2014, **57**, 1526-1536.
7. G. Henkelman, B. P. Uberuaga and H. Jónsson, *The Journal of Chemical Physics*, 2000, **113**, 9901-9904.

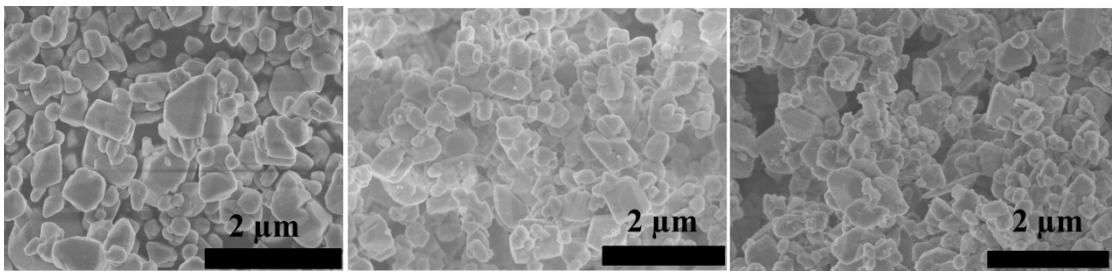

Figure S1. SEM images of the as-prepared samples: (a) LFS, (b) LMFS-2, (c) LMFS-4.

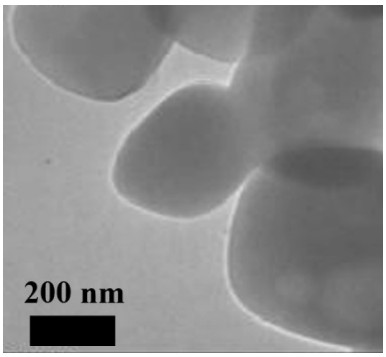

Figure S2. TEM image of LMFS-2 material.

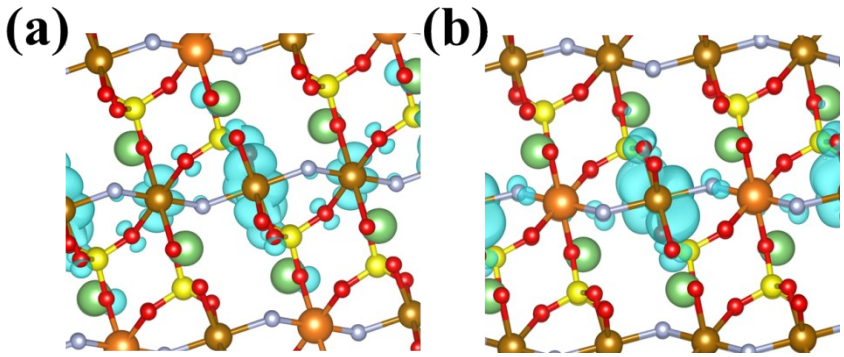

Figure S3. The contour plots of wave functions of the valence band maximum (VBM, a) and conduction band minimum (CBM, b) of Mg-substituted $LiFeSO_4F$.

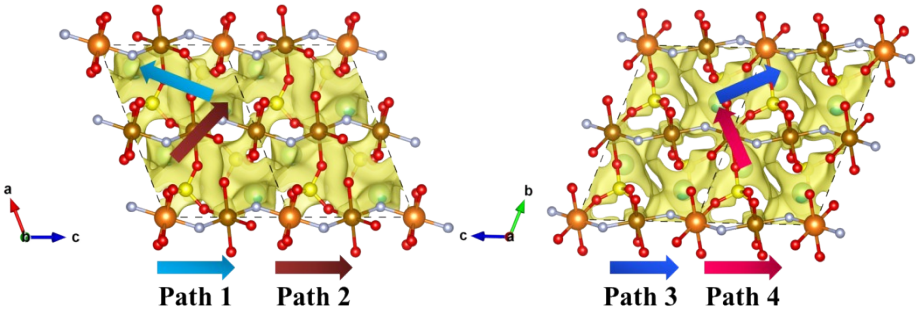

Figure S4. Ion transport path of $LiFeSO_4F$ material.

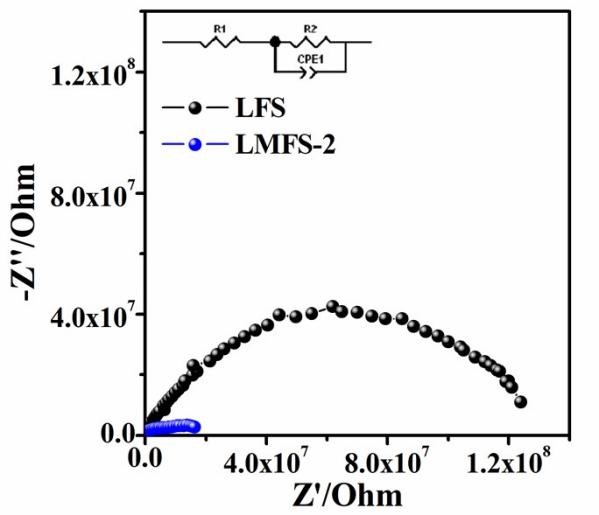

Figure S5. AC impedance spectroscopy of the LFS and LMFS-2 samples

Table S1. The Wyckoff sites of atom in $LiFeSO_4F$ unit cell.

	x	y	z	Occ.	Wyckoff Site
Li	0.270	0.629	0.759	1	2i
S	0.323	0.634	0.250	1	2i
O	0.102	0.643	0.344	1	2i
O	0.278	0.769	0.102	1	2i
O	0.320	0.358	0.146	1	2i
O	0.400	0.251	0.589	1	2i
F	0.126	0.917	0.757	1	2i
Fe	0	0	0	1	1a
Fe	0	0	0.5	1	1b

Table S2. The lattice constants of $LiFeSO_4F$ and Mg-substituted $LiFeSO_4F$.

	a (Å)	b (Å)	c (Å)	α (°)	β (°)	γ (°)
$LiFeSO_4F$ (2×2*1 supercell)	10.442	11.076	7.388	107.074	106.441	98.476
$LiFe_{0.875}Mg_{0.125}SO_4F$	10.374	11.017	7.276	106.753	107.459	97.894

Table S3 The electrochemical properties of $LiFeSO_4F$ with different ions substitution

	Capacity	Voltage	Cycle Performacnce	Rate Performance	Structure	Method
Pristine $LiFeSO_4F$[20]	0.05C 92 mAh g^{-1}	3.34 V	0.2C, After 100 cycles, 34.5mAh g^{-1}	0.2C, 36 mAh g^{-1} 0.5C, 11 mAh g^{-1} 1C, 6 mAh g^{-1}	tavorite	solvothermal
$LiNi_xFe_{1-x}SO_4F$[9]	x = 0.1, 0.1 C, 0.6 Li (~90 mAh g^{-1}), decreasing with the Ni content increase,	3.6 V	No decaying after 25 cycles at 0.1 C	~	triclinic	ionothermal
$LiCo_xFe_{1-x}SO_4F$[9]	X = 0.1, 0.1 C, 0.6 Li (~90 mAh g^{-1}), decaying with the Co content increase,	3.6 V	No decaying after 25 cycles at 0.1 C	~	triclinic	ionothermal
$LiMn_xFe_{1-x}SO_4F$[21]	X = 0.1, 0.05 C, 120 mAh g^{-1}	3.9 V	No decaying after 26 cycles at 0.05 C	~	monoclinic	ionothermal
$LiZn_xFe_{1-x}SO_4F$[10]	Sillimanote (20% Zn), 1/15 C， 0.65 Li (~98.15 mAh g^{-1}) Triplite (10% Zn), 1/15 C, 0.55	3.6V for sillimanite, 3.9V for triplite	~	~	x < 0.05, tavorite, 0.05<x<0.15 triplite x>0.15 sillimanite	ceramic

	Li(~82.5 mAh g^{-1})					
$LiTi_xFe_{1-x}SO_4F$[11]	x= 0.02, 0.1 C, 124.8 mAh g^{-1},	3.6 V	0.1 C, after 100 cycles 102.5 mAh g^{-1}	1 C, 43 mAh g^{1}, 2 C 24.4 mAh g^{-1},	tavorite	solvotherm al
$LiMg_xFe_{1-x}SO_4F$ (This work)	x = 0.02, 0.1 C, 101.1 mAh g-1	3.6 V	0.1 C, after 100 cycles 89 mAh g^{-1}	1 C, 33.3 mAh g^{1}, 2 C 16.8 mAh g^{-1},	tavorite	solvotherm al

Table S4. The concentration of the Li, Fe, Mg element after cycle.

Element	Concentartion (mg/L)	Relative Standard Deviation (RSD%)	Standard Deviation (SD%)
Li	409.685	0.9	3.64532
Fe	0.001451	10.6	0.003836
Mg	0.026860	3.8	0.013950